Nanotechnology Perceptions
ISSN 1660-6795
www.nano-ntp.com

Investigation of Machining Characteristics of AA7050/Gr/CNT Composites

Nagaraja T. K.[1], Sasidhar Jangam[2]

[1]Research Scholar, Department of Mechanical and Automobile Engineering, School of Engineering and Technology, CHRIST (Deemed to be University), Bangalore, Karnataka, India, nagaraja.tk@res.christuniversity.in
[2]Assistant Professor, Department of Mechanical and Automobile Engineering, School of Engineering and Technology, CHRIST (Deemed to be University), Bangalore, Karnataka India, sasidhar.jangam@christuniversity.in

In this investigation, an effort was made to use the Electric Discharge Machining (EDM) technology to process the hybrid composites AA7050/Gr/CNT. The tool wear ratio (TWR), material removal rate (MRR) and surface roughness (Ra) were detailed as outcomes. The experimental runs were planned exploiting the Taguchi mixed orthogonal array. The composites were made through the stir casting technique and machined by varying current, tool materials, powder concentration, and pulse on time. The results showed that improvement in MRR was due to the bridging effect, TWR depends on the physical property of the electrode and Ra depends on the flushing of the machined debris. The densification of plasma channel and machined debris occurred at the higher parametric value of current and Pulse on time. The microstructure of samples machined with a brass tool exhibited cracks, craters, globules, remelted layers, and black spots, indicating thermal and chemical effects of the EDM process, while aluminum tool machining showed deeper craters, uneven surfaces, and clustered globules, attributed to aluminum's properties affecting material removal and solidification behavior, whereas Copper tool machining resulted in larger globules due to its high thermal conductivity, along with craters, pinholes, remelted material, cracks, and pits. The ANOVA table revealed that Pulse on was the supreme process parameters trailed by the powder concentration. The PROMTHEE revelaed that with 5% Al2O3 integrated dielectric medium, composites machined with 7A current and 20µs Tonne using the brass tool provided the best machining performance.

Keywords: Hybrid composites; PMEDM; Optimization; ANOVA;

PROMTHEE.

1. Introduction

Composites with a high endurance-to-weight ratio were projected to be a viable option for aviation, maritime, and security applications [1]. In-situ fabrication, Powder metallurgy and casting were the diverse techniques used to produce composites [2-4]. The prime method for manufacturing composites at a minimal cost was liquid stir casting technique. The most challenging task in composite production was attaining homogenous dispersion of reinforced particles [5,6]. Preheated particles were mixed in the furnace utilizing a mechanical agitator for the specified period at a persistent speed to attain uniform dispersion [7,8]. Traditional machining of composites was tedious task owing to the existence of hard reinforcement particles, which instigates significant tool wear [9]. To solve the issue, composites were processed exploiting an unconventional machining process [10], which includes abrasive jet machining, ultrasonic machining, EDM and electron beam machining, of which EDM machined the composites with extreme accuracy and precision [11].

The distinct input variables which has influence on machining characteristics were Pulse on Time (Ton), Pulse off Time (Toff), machining distance, current and voltage, of which current and Ton were the most influential variables. Torres, A. et al. [12] explored the impact of electrical variables on MRR, TWR, and Ra on Inconel compound. The dielectric fluid was mineral oil has a sparkle point of 82^{o}C, and the cathode material was copper. Positive extremity lead to increased MRR, whilst negative extremity points lead to inferior SR values. Yan Cherng Lin et al. [13] investigated the influence of process variables on MRR and TWR in EDM of SKH 57 high-speed steel utilising copper electrodes. MRR increased in tandem with Ip, peaking at around 100μs Ton, MRR reduced as Ton increased. Ranjith et al utilized copper composite as an electrode and concluded that the enhancement in machining characteristics was attained facilitated by the detached reinforced particles [14].

Adding foreign fragments in the insulating medium changes its property and enhancement in MRR was achieved due to the reduction of insulating strength [15]. Jahan et al [16] explored EDM of hardware steel (SKH-51) with graphite nano powder blended dielectric utilizing Gr, Al, and Al2O3 nano powders and made a logical model for EDM instrument. As indicated by Kibria et al [17], boron carbide (B4C) powder blended in with lamp fuel and deionized water further developed miniature execution EDMs essentially. Tan et al [18] investigated molecule mixed EDM's machining execution and took a gander at the recast layer as a response. Ranjith et al [19] analysed EDM of established Titanium utilizing a Al_2O_3 powder blended dielectric. Attaining best from the available alternatives was the tedious and it can be done by the optimization technique [20]. TOPSIS, Grey Relational Analysis, ELECTRE, PROMETHE and multi-objective optimization with discrete alternatives are the various optimization techniques utilized for the mentioned purpose [21-23]. The investigator conducted several experiments incorporating the incorporation of powdered substances into the dielectric fluid, but there was little literature on machining of AA7050/5Gr/5CNT hybrid composites. In this study, Al2O3 particles were included into the dielectric fluid with an objective of improving the machining characteristics of AA7050/5Gr/5CNT hybrid composites. The primary difficulty is the complexity of machining hybrid composites due to

the varied and distinct properties of the constituent materials. In order to optimise the machining process, a literature was used to identify critical process characteristics, viz tool material and machining conditions, and their interaction in impacting MRR, TWR, and Ra. The tests were conducted using different tool materials, current, pulse duration, and powder concentration. An ANOVA table was used to identify the most significant factor. The modified PROMTHEE method was used to optimise the input parameters.

Table 1 – Chemical composition of AA7050 (Spectrum Analysis)

Elements	Al	Cu	Zn	Mg	Mn	Cr
Composition	Balance	4.6	5.4	3.6	0.6	0.1

2. Experimental procedure

AA7050 alloy, as procured from the Panache Industries was used as the matrix materials, possessing the chemical constitution as portrayed in table 1. The alloy was heat up to the temperature of 800^{o}C and the reinforcements Gr and CNT of 5wt% was heated to the charge of 250^{o}C prior to being incorporated into the melt. At 1000 rpm, the blend was agitated using the four-arm mechanical stirrer for the duration of 180s and after the addition of Mg powder flux, it was once again mixed for 120s. The composites were poured into heated mould built of die steel, turned and faced to the height and diameter of 25mm and 10mm respectively. The sample of AA7050 composites and EDM experimental setup was shown in figure 1 and 2 respectively.

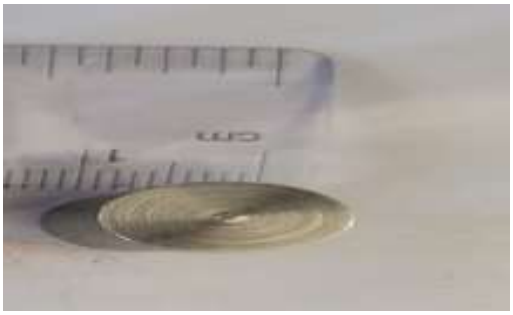

Figure.1 – Sample of AA7050 Composites

Figure.2 – EDM Experimental setup

Table 2 – EDM process parameters and its levels

Input Parameters	Levels
Current (A)	7, 14, 21
Pulse on time (µs) (Ton)	10, 20, 30
Al_2O_3 Powder concentration (g/l)	0, 5
Tool Materials	Brass (1), Copper (2), Aluminium (3)
Work piece	AA7050 hybrid composites
Polarity	Positive
Dielectric medium	Hydro carbon oil
Machined time (Min)	10

Experimental trials were planned using the Taguchi mixed orthogonal array. Positive polarity was consistently maintained throughout the experiment, and hydrocarbon oil was selected as the dielectric fluid. EDM was conducted on the composites using various tool materials (brass, copper, and aluminum), pulse on time, current, and Al2O3 powder concentration, as outlined in Table 2. The performance of the machining was assessed based on MRR, TWR and Ra. Equations 1 and 2 were applied to calculate MRR and TWR. The Ra was measured at ten different locations using a Mitutoyo SJ210 tester, and the mean value was noted. The results were optimized using a modified PROMETHEE approach. The outcomes of the experimental runs are presented in Table 3.

$$MRR = \left(\frac{X_b - X_a}{\rho * z}\right) \text{mm}^3/\text{min} \quad \ldots (1)$$

X_b, X_a – heft of the sample afore and after machining

$$TWR = \left(\frac{Y_b - Y_a}{\rho * z}\right) \text{mm}^3/\text{min} \quad \ldots (2)$$

Y_b, Y_a – heft of the electrode afore and after machining

ρ – Material's density

z – Processed time

Table 3 – EDM Experimental runs and their results

S.No	Powder Concentration (g/l)	Current (A)	Pulse on time (µs)	Tool Materials	MRR (mm^3/min)	TWR (mm^3/min)	Ra (µm)
1	0	7	10	1	0.29272	0.0044	11.7126
2	0	7	20	2	0.25628	0.00196	7.2996
3	0	7	30	3	0.34573	0.0002	9.2402
4	0	14	10	1	0.35636	0.00173	2.1795
5	0	14	20	2	0.55504	0.00371	7.3497
6	0	14	30	3	0.17654	0.00254	5.1643
7	0	21	10	2	0.30236	0.00271	10.5818
8	0	21	20	3	0.41042	0.00153	8.842
9	0	21	30	1	0.26983	0.00126	11.6323
10	5	7	10	3	0.4313	0.00262	13.6035
11	5	7	20	1	0.42626	0.001	6.0495
12	5	7	30	2	0.28576	0.00248	7.5501
13	5	14	10	2	0.39697	0.00294	4.2808
14	5	14	20	3	0.38584	0.00353	5.2274
15	5	14	30	1	0.42198	0.0005	8.5473
16	5	21	10	3	0.30441	0.00321	9.8636
17	5	21	20	1	0.31222	0.00246	5.7402
18	5	21	30	2	0.4526	0.00215	3.9674

3. Results and discussions

Impact of various input variables on MRR.

EDM machining involved melting and evaporating, with the dielectric fluid flushing away machined waste. Figure 1 showed different process factors affected the MRR of composites. Once the powder particles are mixed into the dielectric fluid, the MRR rises and reaches a maximum of 0.40mm3/min when the current is adjusted to 14A. The following facts contributed for the improvement in MRR: (i) when powder particles enter the spark gap, the distance between the electrodes decreases, resulting in a bridging effect that generates heat of higher intensity and increases MRR; (ii) the addition of particles reduces the fluid's dielectric strength, which causes machining cycles to occur more frequently, which in turn improves MRR. The MRR decreases after reaching the 14A saddle point, when the current surges. At the current of 21A densification of the plasma channel happened, which grades in a decline of MMR. This is because the high current causes the heat of high intensity, therefore larger volume of materials removed and MRR increases. In terms of the Tonne, the produced heat was retained inside the spark gap for the required amount of time and removed a higher quantity of material, resulting in a maximum MRR of 0.39mm3/min for 20µs. When the MRR was adjusted to 30µs, removing a larger amount of material causes the machined waste to become denser, which lowers the MRR. Due to the Cu tool's high thermal conductivity, composites machined with it provided a high MRR of 0.37 mm3/min, while composites machined with brass and aluminium tools recorded an MRR of 0.34 mm3/min. Its high thermal conductivity causes it to produce more heat and raises the MRR.

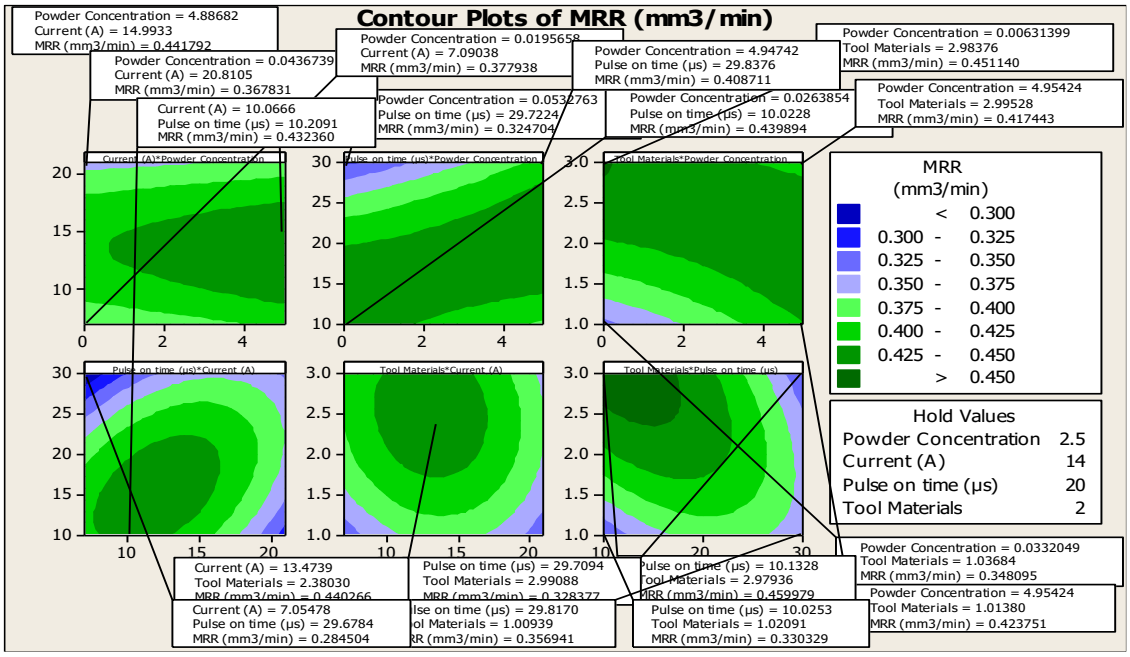

Figure 1 – Effects of various process variables on the MRR of hybrid composites

Under pure dielectric medium, a 7A current yielded an MRR of 0.37mm3/min, which rose to 0.44mm3/min when the current and powder concentration were increased to 14A and 5g/l,

respectively. The MRR for 30µs under pure dielectric medium was 0.32mm3/min, which rose to 0.40mm3/min when 5g/l of powder particles were introduced to the dielectric fluid. The results revealed that irrespective of the process parameter, incorporation of particles increased the MRR, owing to the bridging effect. When brass and Copper was used as the electrode, MRR of 0.34mm^3/min and 0.42mm^3/min was obtained, when 5g/l of Al_2O_3 was added, MRR was raised to 0.42mm^3/min and 0.44mm^3/min. In case of Aluminium electrode, it was reduced from 0.45mm^3/min to 0.41mm^3/min when 5g/l of Al_2O_3 was incorporated in the dielectric medium. From the graph it was confirmed that optimal parametric value of current was 15A, in which maximum MRR was obtained irrespective of tool material utilised for experimentation.

Impact of various input variables on TWR

Incorporation of powder particles has no impact on TWR, as it was slightly increases from 0.0022mm^3/min to 0.0023mm^3/min as depicted in the figure 2. The findings showed that all of the extra heat produced by the bridging effect caused by the inclusion of particles was transferred to the work piece. The current graph exhibited a similar pattern to the MRR, indicating that an increase in current caused the plasma channel to expand, which in turn caused a decrease in TWR. The outcomes verified that both the wok component and the tool materials received some of the heat produced. In contrast to the findings noted by other researchers, the TWR decreases as Tonne increases and reaches a low of 0.0015mm3/min at 30µs Tonne. The interaction impact of the current and Ton was the most influential factor in which minimum TWR was attained when both the parametric values tuned at 7A and 20µs. The copper tool exhibits highest TWR followed by the aluminium and brass electrode. So many researchers claimed that materials with high melting temperature possess least TWR, it was paradoxical to the obtained experimental result. Owing to the high thermal conductivity, Cu conducts higher proportion of the generated heat, hence it exhibits high TWR.

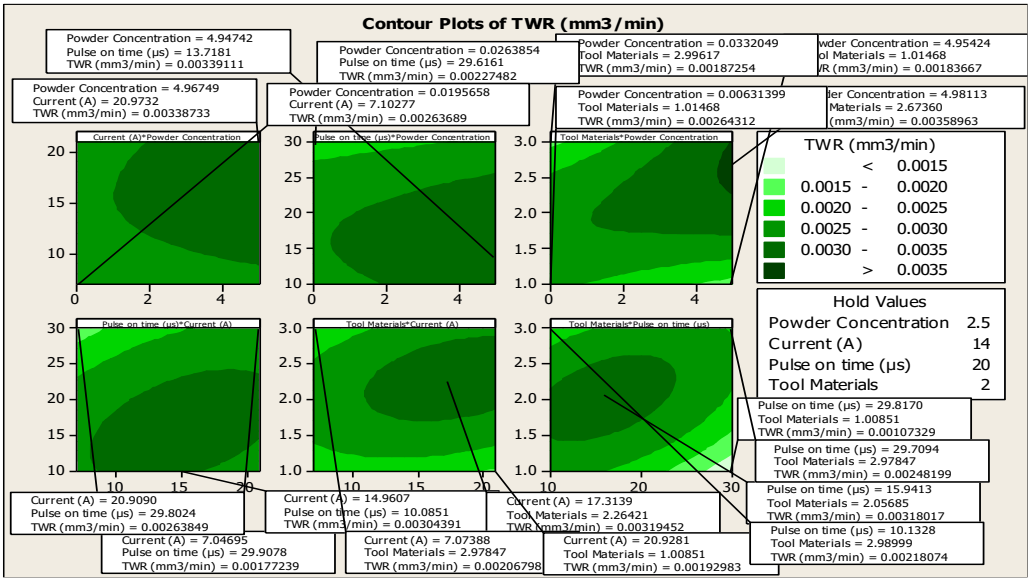

Figure 2 – Effects of various process variables on the TWR of hybrid composites

Impact of various input variables on R_a

The 12.5% improvement in Ra was observed, when the powder particles were incorporated in the dielectric fluid as shown in the figure 3. The enhancement in the surface quality was attributed to the facts (i) as discussed incorporation of particles enables bridging effect, hence to maintain the spark gap, the distance between the electrodes increases which facilitates flushing of machined debris hence Ra decreases. (ii) The presence of particles expedites the uniform heat distribution; hence heat bombard the surface uniformly eliminates uneven machined surface results in improvement of surface quality. The average Ra of 5.45µm was observed when the current was tuned at 14A and it was drastically increased to 8.43µm, when there was rise in current to 21A. The reduction of quality was due to the fact owing to the plasma densification, resolidified layers were formed on the surface. At lower current of 7A, the heat generated was not sufficient to leads to the formation of surface dooms results in reduction of surface quality. The minimum Ra was attained for the Ton value of 20µs, beyond that value owing to the machined debris densification, sedimentation of these particles on the surface occurred leads to the worsening of the surface quality. Of the distinct tool materials used, composites machined using the copper tool exhibit the least Ra value which was attributed to the thermal conductivity of the material.

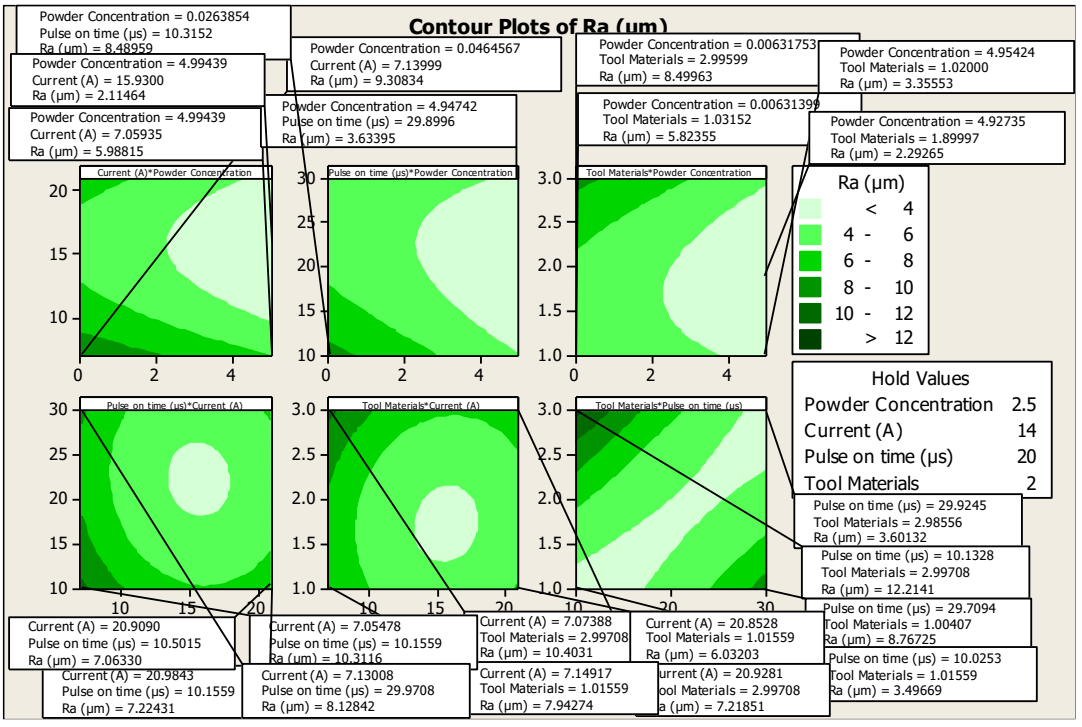

Figure 3 – Effects of various process variables on the R_a of hybrid composites

When the input variables of current and Pulse on time was regulated at 15A and 20µs, without the incorporation of powder Ra of 5.51µm and 5.65µm was obtained and it was drastically reduced to 2.11µm and 2.30µm when 5g/l of Al_2O_3 particles was incorporated in the dielectric fluid, in the above cases copper was used as the tool material. With the

incorporation of Al_2O_3 particles, the best and worst surface quality of 2.28µm and 7.10µm was obtained when copper and aluminium was utilized as the electrode.

Machined Surface Morphology

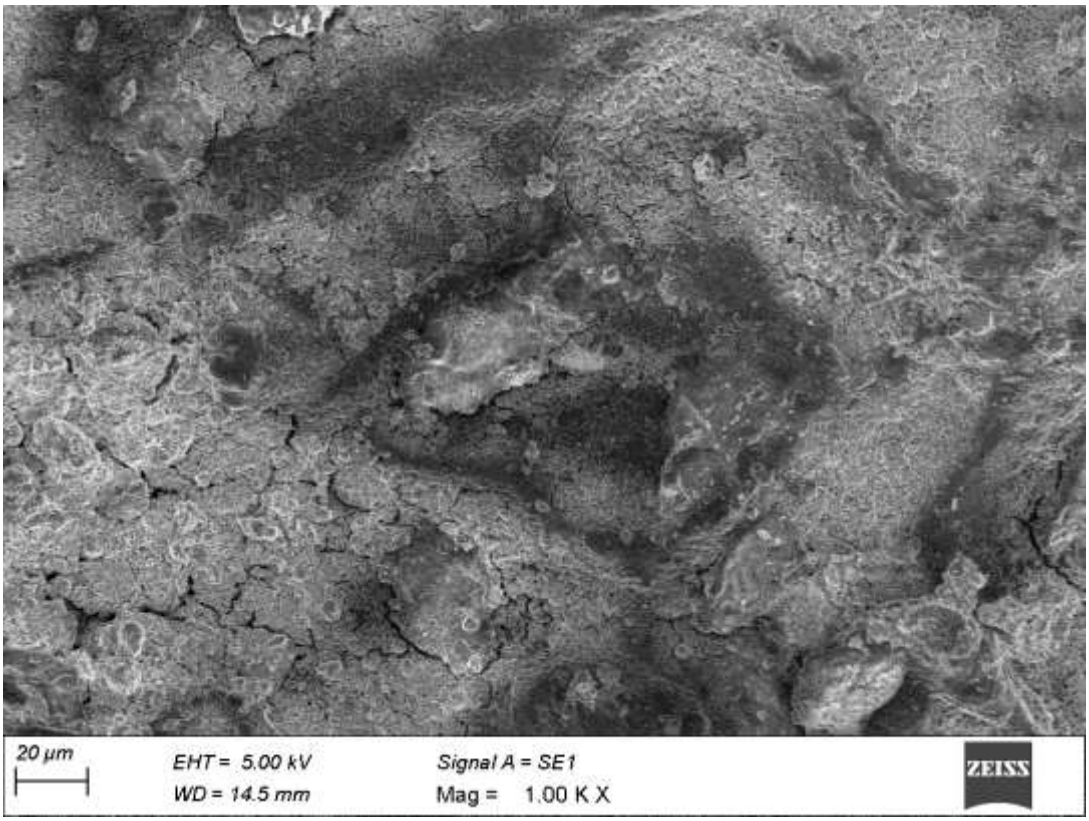

Figure 4 - Surface topography of AA7050 hybrid composites machined with Brass tool.

The microstructure of (EDM) samples machined with a brass tool reveals several distinctive features as shown in figure 4. Cracks are observed, originating from discrete points and converging towards a common point, suggesting a directional influence on crack propagation likely related to the tool-electrode geometry and the EDM process parameters. These cracks result from thermal stresses induced during the rapid heating and cooling cycles characteristic of EDM. The presence of craters indicated the localized material removal, typically associated with the dislodging of molten material or debris from the workpiece surface due to the high-energy electrical discharges. These features are often accompanied by the presence of globules, which are likely formed from the melted material that re-solidifies in small droplet shapes upon cooling. The formation of remelted layers further supports the intense thermal nature of the EDM process, where material is melted and subsequently solidified, potentially leading to altered material properties in these regions. The occurrence of black spots suggests localized chemical changes, such as oxidation, induced by the EDM process.

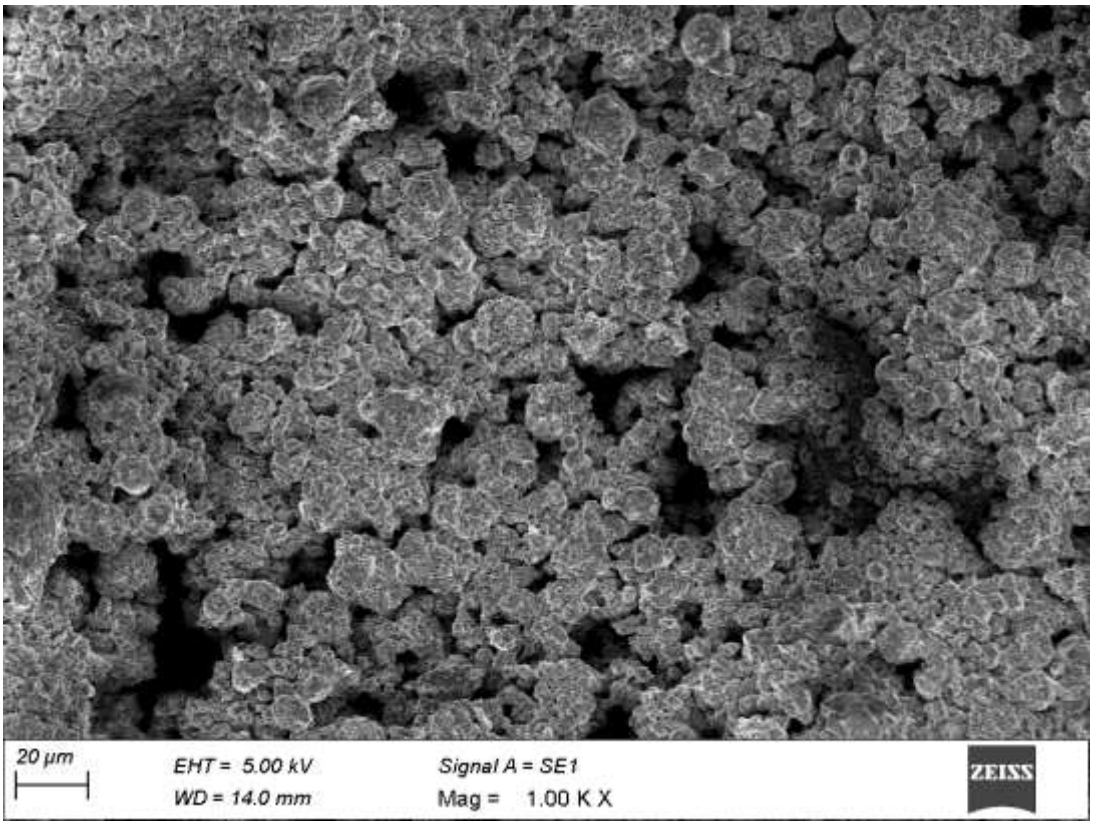

Figure 5 - Surface topography of AA7050 hybrid composites machined with Aluminium tool

Deeper craters are evident as shown in figure5, indicating more significant material removal compared to brass tool machining. The uneven machined surface suggests variations in the material removal rate across the workpiece, possibly due to differences in tool wear associated with the aluminum tool. A notable observation is the presence of a bunch of globules that appear to be sticking together. These globules are likely formed from molten material during the EDM process and have coalesced upon solidification, forming clusters. Aluminum's relatively low melting point and high thermal conductivity lead to rapid solidification of the molten material. As these globules solidify, their close proximity and the rapid cooling process promote their aggregation, forming clusters Cracks are also observed in the microstructure, although the nature and extent of cracking may vary compared to machining with a brass tool. The presence of cracks can be attributed to thermal stresses induced during the EDM process, especially considering the rapid and localized heating and cooling cycles involved.

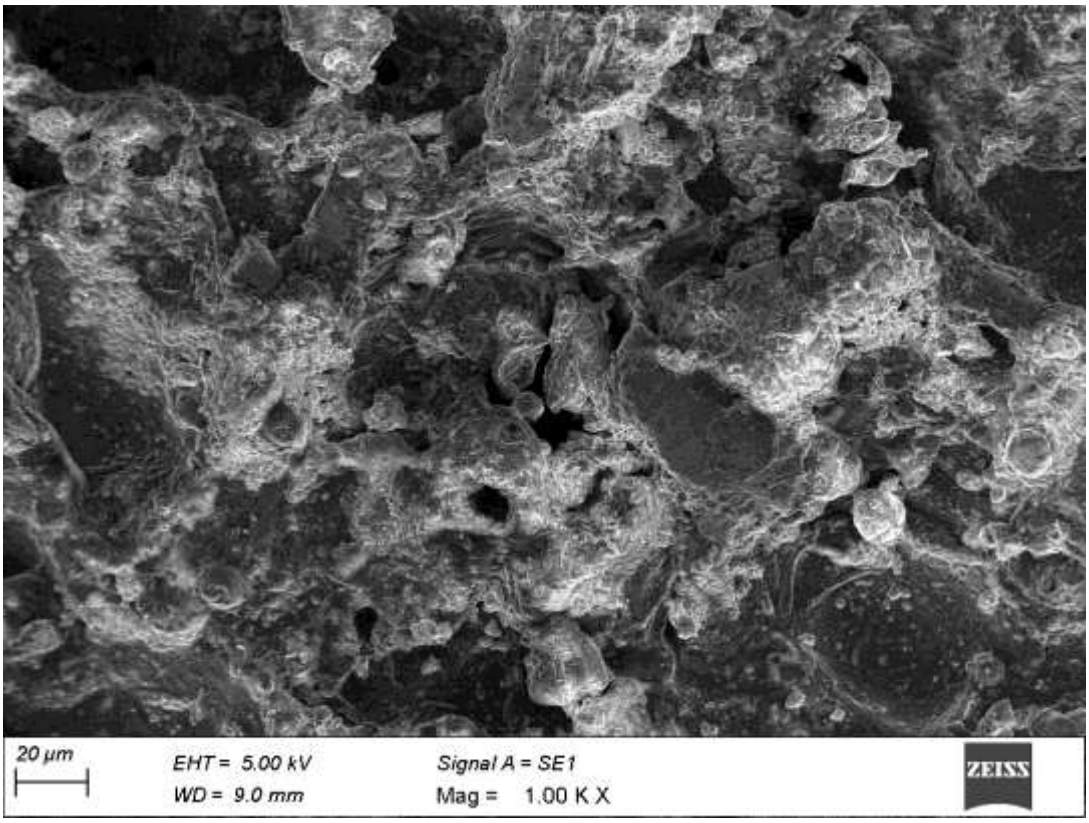

Figure 6 - Surface topography of AA7050 hybrid composites machined with Copper tool.

Globules with an average size of 20µm are dispersed throughout the microstructure, likely formed from molten material during the intense electrical discharges characteristic of EDM as depicted in figure 6. Copper has a higher thermal conductivity compared to other tool materials, which allows for more efficient heat dissipation during the EDM process. This results in a larger heat-affected zone and a more substantial volume of molten material, leading to the formation of larger globules upon solidification. Craters are observed, suggesting localized material removal during the EDM process. The presence of pinholes, small voids also noted, which was attributed to gas evolution or vaporization of material during the discharge phase. These pinholes can affect the surface integrity and dimensional accuracy of the machined component. Remelted material is evident in the microstructure, indicating areas where material has been melted and subsequently solidified. The formation of remelted layers is typical in EDM processes due to the high temperatures generated during electrical discharges. Cracks and pits are observed which can compromise the mechanical properties and dimensional accuracy of the machined component.

ANOVA

The most impactful variable component which sway the machining characteristics of the composites were portrayed in the table 4. It was exposed that Ton was the most persuasive in case of MRR and TWR. From the experimental results it was noticed that there was impact

in machining rate with the changeover Ton. Powder concentration and tool materials have the second greatest influence on MRR and TWR, respectively. With the incorporation of powder the rise in MRR and TWR depends on the properties of the materials used. The following variable which impacts the machining characteristics was current. The outcomes uncovered that incorporation of Al2O3 particles further increases machining performance and surface quality depends on the current and Ton.

Table 4 - Identifying most influential process parameters using Taguchi analysis

ANOVA table for MRR (mm^3/min)				
Level	Powder Concentration	Current (A)	Pulse on time (µs)	Tool materials
1	0.3295	0.3397	0.3474	0.3466
2	0.3797	0.3821	0.3910	0.3748
3		0.3420	0.3254	0.3424
Delta	0.0502	0.0424	0.0656	0.0325
Rank	2	3	1	4
ANOVA table for TWR (mm3/min)				
1	0.002226	0.002108	0.002934	0.001891
2	0.002321	0.002494	0.002365	0.002658
3		0.002218	0.001522	0.002271
Delta	0.000095	0.000387	0.001412	0.000766
-Rank	4	3	1	2
ANOVA table for Ra (µm)				
1	8.222	9.243	8.704	7.644
2	7.203	5.458	6.751	6.838
3		8.438	7.684	8.657
Delta	1.019	3.784	1.952	1.819
Rank	4	1	2	3

For MRR, the regression model indicates that Powder Concentration, Tool Materials, and the interaction term between Current and Tool Materials have statistically significant effects on MRR as depicted in table 5. The negative coefficient for Current suggests a decreasing trend, while the positive coefficients for Powder Concentration and the interaction term indicate an increasing impact on MRR. In the case of TWR, the regression model reveals that Powder Concentration, Tool Materials, and the interaction term between Powder Concentration and Pulse on time significantly influence TWR. The positive coefficients for Powder Concentration and the interaction term suggest an increasing trend in TWR, while the negative coefficient for Tool Materials indicates a decreasing impact. Surface Roughness (Ra) analysis indicates that Tool Materials, the interaction term between Pulse on time and Tool Materials, and the interaction term between Powder Concentration and Pulse on time significantly impact Ra. The positive coefficient for Tool Materials implies an increasing effect on Ra, while the negative coefficients for the interaction terms suggest decreasing impacts.

Modified PROMTHEE approach

The optimal parametric combination as well as the best alternatives were determined using a modified PROMTHEE technique. The first step of the method focuses on determining the optimum parametric combination, while the second phase focuses on determining the best tool materials. The technique initiates with the formation of the decision matrix, as a total of 18 experiments runs were conducted and three response was utilized for the accessing the performance, a decisive matrix of 18X3 was formed as depicted in the equation 3. Subsequently, a weighted and normalised decisive matrix was generated. Equation 4

illustrates that, for beneficiary qualities, this matrix was equal to the ratio of the difference between the row's minimum and maximum elements to the row's ith element. For the non-beneficiary characteristics, Equation 5 illustrates the proportion of the variance between the maxima and ith element relative to the difference between the maxima and minima elements

$$Y_{ij} = \begin{pmatrix} Y_{11} & \cdots & \vdots \\ Y_{21} & Y_{22} & Y_{ni} \\ Y_{jn} & \cdots & Y_{nn} \end{pmatrix} \quad \ldots (3)$$

For beneficiaries

$$A_{ij} = \sum_{i=0}^{n} \frac{(Y_{ij} - Y_{min})}{Y_{max} - Y_{min}} \quad \ldots (4)$$

For non-beneficiaries

$$A_{ij} = \sum_{i=0}^{n} \frac{(Y_{max} - Y_{ij})}{Y_{max} - Y_{min}} \quad \ldots (5)$$

$$B_{ij} = \sqrt{\sum_{j=0}^{n} A_{ij}} \quad \ldots (6)$$

Table 5 – Identification of best parametric combination using modified PROMTHEE optimization technique

Normalised decision matrix			Weighted Normalised decision matrix			Assessment Value	Rank
MRR (mm^3/min)	TWR (mm^3/min)	Ra (µm)	MRR (mm^3/min)	TWR (mm^3/min)	Ra (µm)		
0.306942177	0	0.16552	0.101290918	0	0.0562768	0.396948	18
0.210658973	0.581322216	0.551812	0.069517461	0.191836331	0.1876161	0.670052	11
0.447001041	1	0.381942	0.147510344	0.33	0.1298601	0.77934	5
0.47509366	0.634830256	1	0.156780908	0.209493985	0.34	0.840402	2
1	0.16276355	0.547426	0.33	0.053711971	0.186125	0.754875	8
0	0.441453246	0.738725	0	0.145679571	0.2511667	0.629957	13
0.332416552	0.402692079	0.264505	0.109697462	0.132888386	0.0899315	0.576643	16
0.617918721	0.682239428	0.416798	0.203913178	0.225139011	0.1417113	0.755489	7
0.246461012	0.747659321	0.172549	0.081332134	0.246727576	0.0586667	0.621873	14
0.673063002	0.423847528	0	0.222110791	0.139869684	0	0.601648	15
0.65977099	0.808767123	0.661239	0.217724427	0.266893151	0.2248214	0.842282	1
0.28856163	0.457367481	0.529884	0.095225338	0.150931269	0.1801607	0.65293	12
0.582386168	0.345824896	0.816063	0.192187436	0.114122216	0.2774613	0.764049	6
0.552977823	0.206456224	0.733202	0.182482682	0.068130554	0.2492887	0.707037	10
0.648457852	0.927361525	0.442595	0.213991091	0.306029303	0.1504821	0.818842	4
0.337822129	0.283311495	0.327372	0.111481302	0.093492793	0.1113065	0.562388	17
0.358458961	0.461703395	0.688314	0.118291457	0.15236212	0.2340268	0.710409	9
0.729351278	0.535104229	0.843496	0.240685922	0.176584395	0.2867887	0.839082	3
Weight			0.33	0.33	0.34		

The next step was the formation of the assessment value which is the sum of the square root of all the i^{th} element of the column as shown in the equation 6. The subsequent stage was the formation of relative lattice (Mij) as portrayed in equation 7. Now, the exhibition of every option was contrasted with each other. The distinction between the exhibition of nth option was contrasted and everything different other options and its worth was portrayed in the table 5. The list esteem network was the capacity of correlation lattice as portrayed in the equation 8. At the point when the values of the components in the relative grid was over zero

then a similar worth being placed in file esteem framework, in the event that it is lesser or equivalent to zero, the worth was taken as zero [26] as portrayed in condition 9.

$$D_{ij} = \sum_{i,j=1}^{n} \begin{cases} A_j(1,1) - A_j(2,1) \\ A_j(i,1) - A_j(i,n) \end{cases} \quad \ldots (7)$$

$$C_{ij} = F_j[D_j(a,b)] \quad \ldots (8)$$

$$C_{ij} = \begin{cases} 0, & D_{ij} \leq 0 \\ D_{ij}, & D_{ij} > 0 \end{cases} \quad \ldots (9)$$

Table 6 – Comparison of tool performance using modified PROMTHEE optimization technique

	Tool Materials	Brass	Copper	Aluminium	Leaving flow	Leaving flow	Entering flow	Net flow	Rank
a1	Copper	0	0.48	0.394	0.291333	0.291	0.146	0.145667	2
a2	Brass	0.437	0	0.67	0.369	0.369	0.215	0.153667	1
a3	Aluminium	0	0.166	0	0.055333	0.055	0.355	-0.29933	3
	Entering flow	0.145667	0.215333	0.354667					

The weights of each condition were compounded to create a weighted index value after the index value was calculated, as stated in equation 10. The aggregate index was then calculated as the total of these index values, which are displayed in table 6. The next step was to generate the matrix of the arriving and outgoing flows according to equation 12. The average values of the rows and columns—also known as the incoming and departing flows—are then calculated [27]. The net flow value was determined by subtracting the outgoing flow from the incoming flow [28]. The optimal choice was determined to be the one with the highest net flow value.

$$E_{ij} = W_{ij} \sum_{i=0}^{n} C_{ij} \quad \ldots (10)$$

$$F_{ij} = SUM\ (D_{ij}) \quad \ldots (11)$$

$$Z_{ij} = \begin{pmatrix} 0 & F_{12} & F_{in} \\ F_{21} & 0 & \vdots \\ F_{nj} & \cdots & 0 \end{pmatrix} \quad \ldots (12)$$

4. Conclusion

1) The MRR increases with the addition of powder particles owing to the bridging effect, and reduction in Ra value was due to the complete flushing of particles because of increased spark gap. The reduction of TWR was attributed to the electrical conductivity of the electrodes used. The most influential process parameters were identified using the ANOVA table, it was revealed that Ton was the most impactful process parameters followed by the powder concentration and current.

2) The microstructure analysis of samples machined with different tool materials revealed distinct characteristics. Brass tool machining exhibited cracks, craters, globules, remelted layers, and black spots, indicating thermal and chemical effects of the EDM process. Aluminum tool machining resulted in deeper craters, uneven surfaces, and clustered

globules, which can be attributed to aluminum's properties affecting material removal and solidification behavior. Copper tool machining showed larger globules, along with craters, pinholes, remelted material, cracks, and pits, which can be attributed to its high thermal conductivity.

3) The composites machined with 7A current, 20µs Ton under 5% Al2O3 incorporated dielectric medium using the brass tool proffered best machining performance. The performance of the tool was contrasted using modified PROMTHEE approach, it was found that the copper was the best tool followed by brass and aluminium. Powder Concentration, Tool Materials, and their interactions emerge as key contributors, providing actionable insights for optimizing the EDM process and enhancing machining performance.

Future Scope

Future study should focus on investigating improved machining processes, adding more particles to the composite matrix, and evaluating the environmental effect of machining. Enhancing surface finish, validating in practical applications, and creating models for predictive simulations are crucial areas for future research.

References

1. Garg, P., Jamwal, A., Kumar, D., Sadasivuni, K. K., Hussain, C. M., & Gupta, P. (2019). Advance research progresses in aluminium matrix composites: manufacturing & applications. Journal of Materials Research and Technology, 8(5), 4924-4939.
2. Sudha, G. T., Stalin, B., Ravichandran, M., & Balasubramanian, M. (2020). Mechanical properties, characterization and wear behavior of powder metallurgy composites-a review. Materials Today: Proceedings, 22, 2582-2596.
3. Singh, H., Haq, M. I. U., & Raina, A. (2020). Dry sliding friction and wear behaviour of AA6082-TiB2 in situ composites. Silicon, 12(6), 1469-1479.
4. TK, Nagaraj., & Jangam, S. (2023). Developing a steady state wear equation for AA7050 hybrid composites/steel interface at elevated temperature. Advances in Materials and Processing Technologies, 1-16.
5. Kareem, A., Qudeiri, J. A., Abdudeen, A., Ahammed, T., & Ziout, A. (2021). A review on AA 6061 metal matrix composites produced by stir casting. Materials, 14(1), 175.
6. Rajamanickam, R., & Giridharan, P. K. (2015). Experimental investigation of surface hardness and dry sliding wear behavior of AA7050/B 4 C p. High Temperature Material Processes: An International Quarterly of High-Technology Plasma Processes, 19(3-4).
7. Singhal, C., Murtaza, Q., Alam, P., & Hasan, F. (2019). Structural and mechanical properties of microwave hybrid sintered aluminium silicon carbide composite. Advances in Materials and Processing Technologies, 5(4), 559-567.
8. Ranjith, R., Giridharan, P. K., Devaraj, J., & Bharath, V. (2017). Influence of titanium-coated (B4Cp+ SiCp) particles on sulphide stress corrosion and wear behaviour of AA7050 hybrid composites (for MLG link). Journal of the Australian Ceramic Society, 53(2), 1017-1025.
9. Vigneshwaran, S., John, K. M., Deepak Joel Johnson, R., Uthayakumar, M., Arumugaprabu, V., & Kumaran, S. T. (2021). Conventional and unconventional machining performance of natural fibre-reinforced polymer composites: A review. Journal of Reinforced Plastics and Composites, 40(15-16), 553-567.
10. Prabhakar, M., Ranjith, R., & Venkatesan, S. (2021). Characterization of electric discharge

machining of titanium alloy utilizing MEIOT technique for orthopedic implants. Materials Research Express, 8(8), 086505.

11. Singh Bains, P., Sidhu, S. S., & Payal, H. S. (2018). Investigation of magnetic field-assisted EDM of composites. Materials and Manufacturing Processes, 33(6), 670-675.
12. Torres, A., Luis, C. J., & Puertas, I. (2015). Analysis of the influence of EDM parameters on surface finish, material removal rate, and electrode wear of an INCONEL 600 alloy. The International Journal of Advanced Manufacturing Technology, 80(1), 123-140.
13. Lin, Y. C., Yan, B. H., & Chang, Y. S. (2000). Machining characteristics of titanium alloy (Ti–6Al–4V) using a combination process of EDM with USM. Journal of Materials Processing Technology, 104(3), 171-177.
14. Somu, C., Ranjith, R., Giridharan, P. K., & Ramu, M. (2021). A novel Cu-Gr composite electrode development for electric discharge machining of Inconel 718 alloy. Surface Topography: Metrology and Properties, 9(3), 035025.
15. Philip, J. T., Mathew, J., & Kuriachen, B. (2021). Transition from EDM to PMEDM–impact of suspended particulates in the dielectric on Ti6Al4V and other distinct material surfaces: a review. Journal of Manufacturing Processes, 64, 1105-1142.
16. Jahan, M. P., Rahman, M., & Wong, Y. S. (2011). A review on the conventional and micro-electrodischarge machining of tungsten carbide. International journal of machine tools and manufacture, 51(12), 837-858.
17. Kibria, G., Shivakoti, I., & Bhattacharyya, B. (2014). Experimentation and analysis into micro-hole machining of Ti-6Al-4V by micro-EDM using boron carbide powder mixed de-ionized water. International Journal of Manufacturing, Materials, and Mechanical Engineering (IJMMME), 4(1), 22-41.
18. Tan, P. C., & Yeo, S. H. (2008). Modelling of overlapping craters in micro-electrical discharge machining. Journal of Physics D: Applied Physics, 41(20), 205302.
19. Ranjith, R., Prabhakar, M., Giridharan, P. K., & Ramu, M. (2021). Influence of Al203 particle mixed dielectric fluid on machining performance of Ti6Al4V. Surface Topography: Metrology and Properties, 9(4), 045052.
20. Ranjith, R., & Vimalkumar, S. N. (2021). Integrated MOORA-ELECTRE approach for solving multi-criteria decision problem. World Journal of Engineering.
21. Rao, R. V., Saroj, A., Ocloń, P., & Taler, J. (2020). Design optimization of heat exchangers with advanced optimization techniques: a review. Archives of Computational Methods in Engineering, 27(2), 517-548.
22. Anoune, K., Bouya, M., Astito, A., & Abdellah, A. B. (2018). Sizing methods and optimization techniques for PV-wind based hybrid renewable energy system: A review. Renewable and Sustainable Energy Reviews, 93, 652-673.
23. Kizielewicz, B., & Sałabun, W. (2020). A new approach to identifying a multi-criteria decision model based on stochastic optimization techniques. Symmetry, 12(9), 1551.